

Fermi National Accelerator Laboratory

FERMILAB-Conf-95/174-E

CDF and DØ

## Photon Production at CDF and DØ

Jodi I. Lamoureux

*Fermi National Accelerator Laboratory  
P.O. Box 500, Batavia, Illinois 60510*

July 1995

Proceedings from the *10th Topical Workshop on Proton-Antiproton Collider Physics*,  
Fermi National Accelerator Laboratory, Batavia, Illinois, May 9-13, 1995.

## **Disclaimer**

*This report was prepared as an account of work sponsored by an agency of the United States Government. Neither the United States Government nor any agency thereof, nor any of their employees, makes any warranty, express or implied, or assumes any legal liability or responsibility for the accuracy, completeness, or usefulness of any information, apparatus, product, or process disclosed, or represents that its use would not infringe privately owned rights. Reference herein to any specific commercial product, process, or service by trade name, trademark, manufacturer, or otherwise, does not necessarily constitute or imply its endorsement, recommendation, or favoring by the United States Government or any agency thereof. The views and opinions of authors expressed herein do not necessarily state or reflect those of the United States Government or any agency thereof.*

## PHOTON PRODUCTION AT CDF AND D0

Presented by Jodi I. Lamoureux

Brandeis University/CDF

P.O. Box 9110

Waltham, Massachusetts 02254

---

Prompt photon production has been studied in  $\bar{p}p$  collisions at  $\sqrt{s} = 1.8$  TeV using the CDF and D0 detectors at Fermilab. The measured inclusive isolated photon spectrum at CDF and D0 are used to test NLO QCD predictions. The CDF result shows that additional soft radiation ( $K_T$ ) in excess of NLO QCD is required to explain the data. No new resonance is observed in the photon + jet mass spectrum from D0 which is consistent with NLO QCD predictions. The pseudorapidity distribution of the leading jet in photon events at CDF is compared to different parton distribution sets. The angular distribution is found to be better explained by a larger Bremsstrahlung contribution.

---

Prompt photon production is studied at the Fermilab Collider in order to test current parton distribution functions and QCD predictions. At lowest order, the Compton process dominates showing that photons are a direct probe of the gluon distribution in the proton. To test current QCD predictions, comparisons are made between data and NLO calculations. In some cases we find that NLO calculations are insufficient to describe the data well and that effects of higher order QCD processes can be observed as additional transverse momentum ( $K_T$ ) in the data. Many of these results were presented previously. (1)

## I. INCLUSIVE ISOLATED PHOTON PRODUCTION

### A. Event Selection and Background Subtraction

To measure prompt photons both CDF and D0 (2) employ EM calorimeters segmented into towers in  $\eta\phi$  space. The background from neutral mesons  $\pi^0$ ,  $\eta$  and  $K_S^0$  in jets is suppressed by requiring isolated photon candidates; CDF requires less than 2 GeV in a cone of radius 0.7 in  $\eta\phi$ ; D0 requires less than 2 GeV in the annulus between  $R = 0.2$  and  $R = 0.4$ . Both experiments (CDF,D0) require photon candidates to have little hadronic energy (HAD/Total < 11%, 4%), be neutral (no track, dE/dX separation), have good

shower profile (strip  $\chi^2$ , depth+transverse  $\chi^2$ ), and be central ( $|\eta| < 0.9$ ,  $0.9$ ). Cosmic ray muon bremsstrahlung is rejected with a missing  $E_T$  cut ( $\cancel{E}_T/E_{T\gamma} < 0.8, 0.5$ ). CDF also requires no extra local energy depositions in a strip chamber greater than 1 GeV, and an event vertex within 60 cm of the center of the detector. Both experiments have three trigger thresholds in  $E_T$ . For this analysis CDF uses  $0.06 \text{ pb}^{-1}$  above 6 GeV,  $16 \text{ pb}^{-1}$  above 16 GeV,  $19 \text{ pb}^{-1}$  above 50 GeV and D0 uses  $0.014 \text{ pb}^{-1}$  above 6 GeV,  $0.065 \text{ pb}^{-1}$  above 14 GeV, and  $11.4 \text{ pb}^{-1}$  above 30 GeV. A hardware isolation cut in the CDF trigger makes it possible to acquire more data at low  $P_T$ .

After all cuts, a background predominantly from isolated  $\pi^0$  and  $\eta$  mesons remains. To remove this background one of two methods, a photon conversion probability measure or a photon shower profile measure, are used. (2) The fraction of data which are photons is shown in Figures 1a and 1b as a function of photon  $P_T$ . These fractions are used differently in the CDF and D0 analyses. CDF uses a bin by bin background subtraction in  $P_T$  whereas D0 uses the functional fit shown to subtract the background contribution. Using the D0 method, the CDF statistical uncertainty is reduced by a factor of  $\sim 4$ . D0 has investigated the shape dependent systematic uncertainty in the fit which is correlated bin to bin, but may vary from the minimum shown at low  $P_T$  to the maximum shown at high  $P_T$  or vice versa.

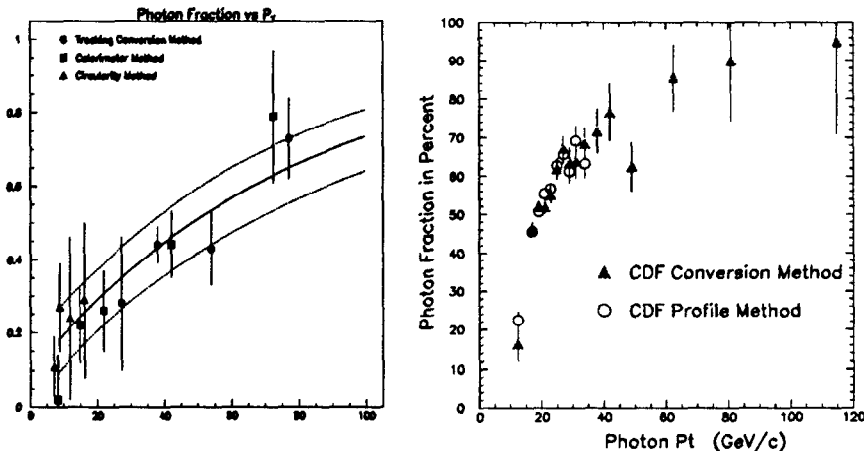


FIG. 1. LEFT TO RIGHT a) The fraction of D0 data which are photons. b) The fraction in percent of CDF data which are photons.

### B. Inclusive Isolated Photon Results

The measured inclusive photon cross section from D0 is shown in Figures 2a and 2b. Good agreement is found between data and the prediction (3) of NLO QCD over almost five orders of magnitude.

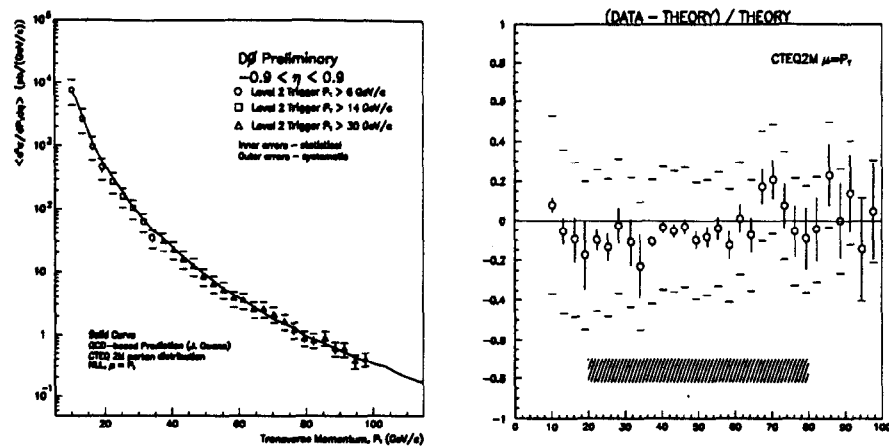


FIG. 2. LEFT TO RIGHT a) D0 inclusive isolated photon cross section b) The fractional difference between the data and NLO QCD prediction.

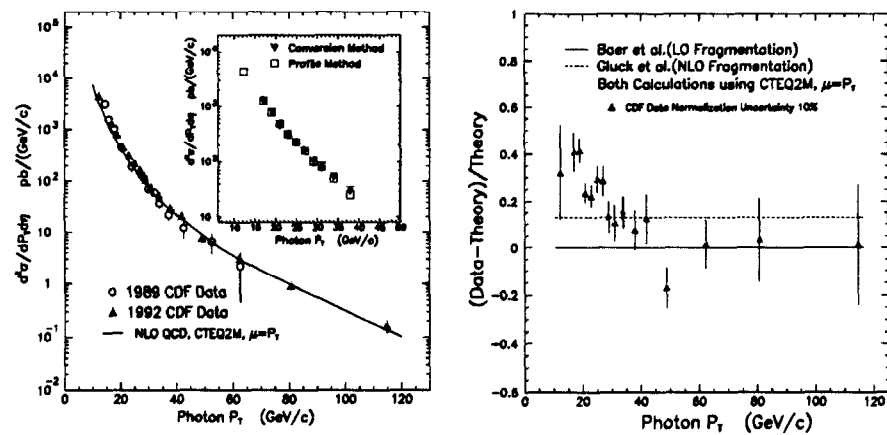


FIG. 3. LEFT TO RIGHT a) CDF inclusive isolated photon cross section b) The fractional difference between the data and NLO QCD prediction.

The same for CDF is shown in Figures 3a and 3b. Although there is qualitative agreement between data and the NLO QCD prediction, the fractional difference between the data and theory show that the data has a steeper slope at low  $P_T$ . Notice that the CDF and D0 measurements are still compatible within the systematic uncertainty. The CDF result has been previously reported (2) and it was shown that current parton distributions and QCD scale do not explain the slope of the data. Figure 3a includes the theoretical prediction of a NLO fragmentation function. (4) Although there is no visible  $P_T$  dependence from the NLO fragmentation function, it is believed that other differences in the calculation cancel out the effect. Consistent definitions for all comparisons leads to a 5% effect at low  $P_T$  (16 GeV/c) which drops to nothing at high  $P_T$ .

Another possible explanation for the excess at low  $P_T$  is that additional soft radiation, beyond NLO QCD, contributes in the form of  $K_T$ . A strong case for additional  $K_T$  has been made in the global analysis of photon data. (5) To investigate the effect of soft radiation, a parton shower has been added to the NLO QCD prediction. Figure 4 shows that the fractional difference between a NLO QCD prediction which includes a parton shower and one without has the same magnitude and shape effect as is observed in the data. Further evidence can be found in the diphoton events at CDF which have  $K_T$  in excess of NLO QCD. (6)

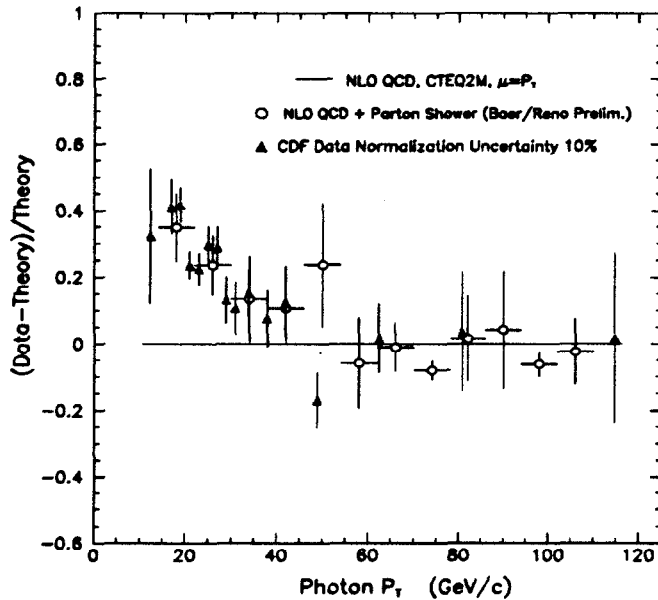


FIG. 4. Open circles are the fractional difference between a NLO QCD prediction which includes a parton shower and one without showing the same size and shape effect as observed in the data.

## II. PHOTON + JET MASS

The invariant mass spectrum for the photon and lead jet can be used to test QCD as well as search for new mass resonances. Data are selected with  $P_T^\gamma > 30$  GeV/c and  $|\eta_J| < 3.5$  at D0. All observed jet clusters more than  $90^\circ$  away in azimuth from the photon were summed and the mass shown in Figure 5 is calculated using photon and jet four-momenta. Good agreement is found with QCD and there is no indication of a statistically significant resonance. A previously reported CDF resonance search (7) found similar results.

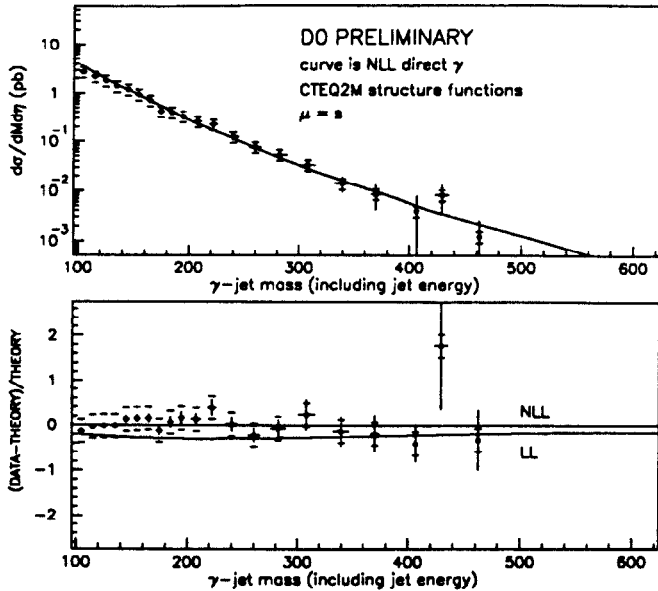


FIG. 5. TOP TO BOTTOM a) The photon and jet mass distribution in D0 events (points) compared to NLO QCD (histogram). b) The fractional difference between the data and NLO QCD.

## III. PHOTON + JET PSEUDORAPIDITY

A measurement of the parton distribution functions which is insensitive to  $K_T$  comes from the jet pseudorapidity distribution in photon events. The CDF conversion background subtraction method is used for photons in the range  $16$  GeV/c  $< P_T^\gamma < 40$  GeV/c where the jet is required to be back to back with the photon,  $150^\circ < \Delta\phi_{\gamma J} < 210^\circ$ . All other cuts are the same as for the inclusive spectrum. The  $\Delta\phi_{\gamma J}$  cut rejects many two jet events. The pseudorapidity distribution is shown in Figure 6a where data have been corrected for detector resolution based on the results of a monte-carlo simulation. In order to compare the shape of the distributions, the theoretical prediction has been normalised to the first bin of the data. Figure 6b is the ratio of data

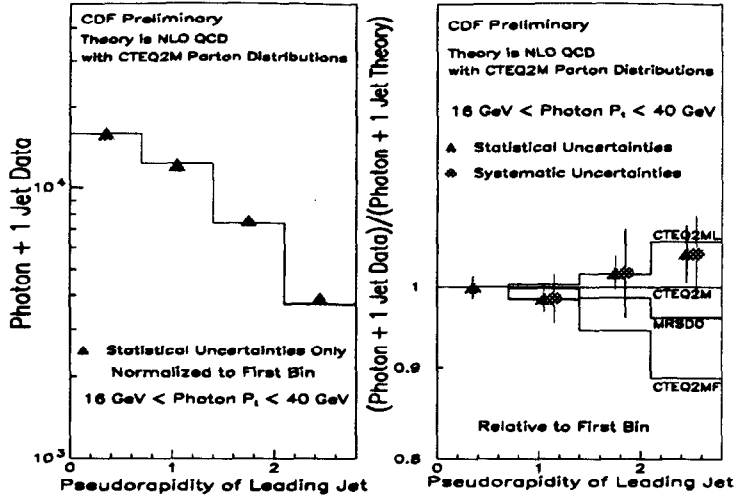


FIG. 6. LEFT TO RIGHT a) The jet pseudorapidity in CDF photon events (points) compared to NLO QCD (histogram). b) The ratio of data to NLO QCD (CTEQ2M) and the ratio of various parton distribution sets to CTEQ2M. Statistical and systematic uncertainties are shown separately.

and theory. The theoretical ratios show that CDF is becoming sensitive to the differences between modern distribution functions.

Since the photons in this analysis are restricted to  $|\eta^\gamma| < .9$ , events with jets at large pseudorapidity are boosted more than events with central jets. Boosted events come from one high  $x$  parton and one low  $x$  parton. The average low  $x$  partons which contribute to each bin in these distributions varies by less than a factor of two whereas the average high  $x$  partons vary by more than a factor of five. Since the observed shapes are due to the high  $x$  partons which are less sensitive to  $K_T$ , this result is essentially independent of  $K_T$ .

#### IV. GAUGE BOSON + JET $\cos\theta^*$ DISTRIBUTION

The  $\cos\theta^*$  distribution is very sensitive to the relative contributions of LO and NLO diagrams. At lowest order,  $u$  and  $t$  channel  $\gamma$  and  $W^\pm$  production are achieved most often through the exchange of a spin 1/2 quark which has a  $1/(1-\cos\theta^*)$  dependence whereas jets are most often produced through the exchange of a spin 1 gluon which has a  $1/(1-\cos\theta^*)^2$  dependence. D0 measures the photon  $\cos\theta^*$  distribution (Figure 7a) using data from the  $P_T^\gamma > 30$  GeV/c trigger. Photons were also restricted to regions of constant acceptance in  $\eta^*$ ,  $\eta^{boost}$ , and  $P^*$ . (8) The neutral meson background ( $\cos\theta^* < 0.6$ ) is  $\sim 48\%$  of the data sample. The measured angular distribution has been corrected for this background by subtracting the expected contribution of dijets. CDF uses the same photon and jet sample as for the jet pseudorapidity measurement. Events are restricted to regions of constant acceptance. (9) This is compared

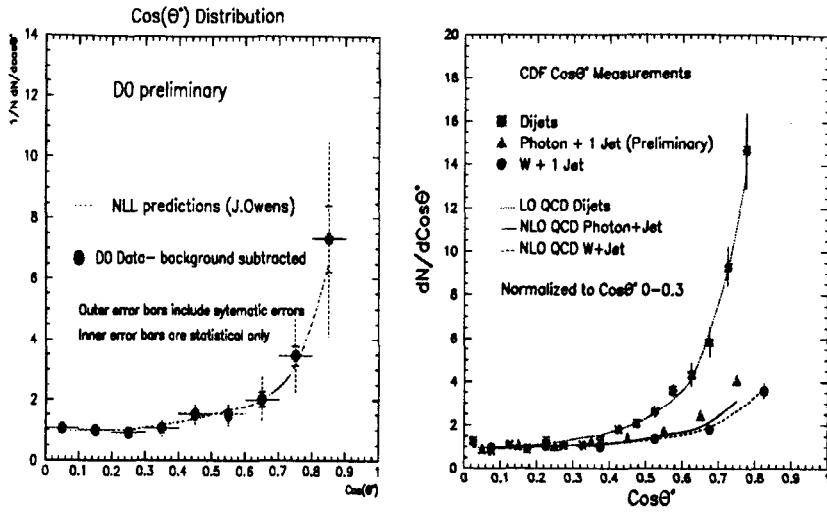


FIG. 7. LEFT TO RIGHT a) D0  $\gamma$  + jet angular distribution. b) CDF angular distributions for dijet,  $\gamma$  + jet, and  $W^\pm$  + jet events are compared to QCD predictions.

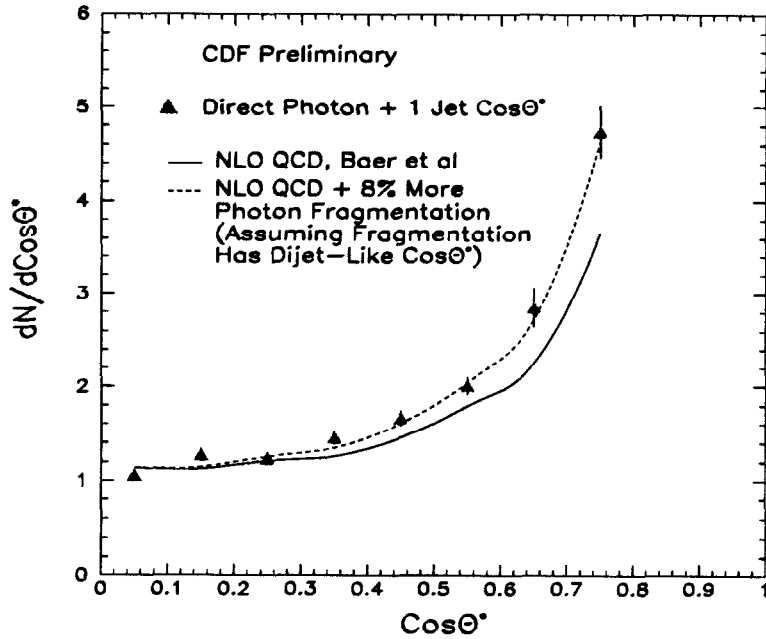


FIG. 8. CDF  $\gamma$  + jet angular distribution compared to NLO QCD with 8% more photon fragmentation.

in Figure 7b to the previously reported dijet and vector boson results. (10) The gluon exchange is clearly visible in the dijet data. The photon data is steeper than NLO theory. The  $W^\pm$  distribution is flatter than the photon distribution because it is produced more often through the  $s$  channel which has no angular dependence.

To investigate the effect of more gluon propagators in the photon distribution, CDF compares the photon data to the sum of the NLO QCD prediction and a dijet component (Figure 8). The best fit for all data is found for 8% more dijet like contribution. It has been suggested that such a contribution may come from NLO photon fragmentation. (4) For the perturbative hard radiative case where two jets are observed in the data, there is agreement between data and LO QCD. Figures 9a and 9b show the  $\cos\theta^*$  distribution of the photon and lead jet when an additional jet is either FAR ( $\Delta\phi_{\gamma J_2} > \pi/2$ ) or NEAR ( $\Delta\phi_{\gamma J_2} < \pi/2$ ) the photon. The NEAR case is more likely photon bremsstrahlung than the FAR case.

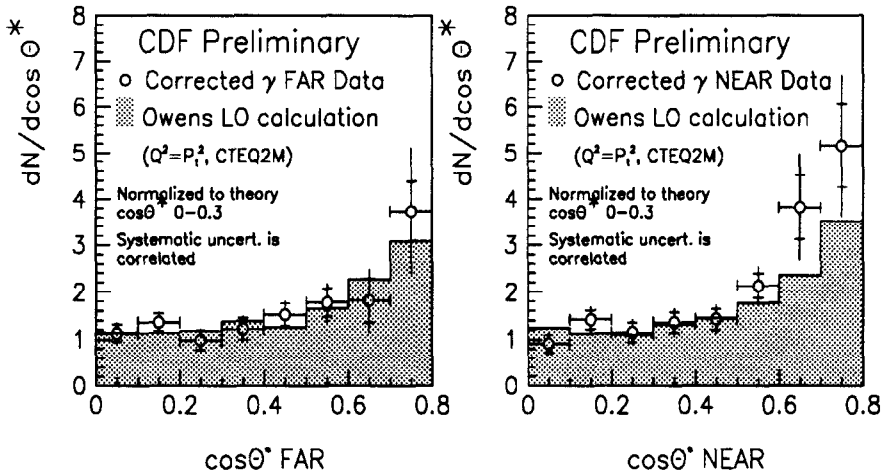


FIG. 9. LEFT TO RIGHT a) CDF  $\gamma$  + lead jet angular distribution in the two jet sample for the FAR region ( $\Delta\phi_{\gamma J_2} > \pi/2$ ) and b) for the NEAR region ( $\Delta\phi_{\gamma J_2} < \pi/2$ ).

## V. CONCLUSIONS

Measurements of prompt photon production at the Fermilab Collider provide precision tests of NLO QCD and constrain the gluon distribution of the proton. We have found that NLO QCD is insufficient to describe the inclusive isolated photon cross section well. We are also becoming sensitive to differences between modern distribution functions with the photon and jet pseudorapidity distribution. The NLO photon fragmentation appears to describe the  $\cos\theta^*$  distribution better than the simpler LO form. In addition,

no evidence is found in the  $\gamma + \text{Jet}$  invariant mass distribution for new resonances.

#### REFERENCES

1. J. Lamoureux (CDF Collaboration), Proceedings of the XXXth Recontres de Moriond (1995), Fermilab-Conf-95/115-E.
2. F. Abe *et al.* (CDF Collaboration), *Phys. Rev. Lett.* **73**(1994)2662; S. Fahey (D0 Collaboration), DPF94, Fermilab-Conf-94/323A-E.
3. H. Baer, J. Ohnemus, and J. F. Owens, *Phys. Lett.* **B234**(1990)127
4. Gluck *et al.*, *Phys. Rev. Lett.* **73**(1994)388.
5. J. Huston *et al.*, MSU-HEP-41027, CTEQ407.
6. R. Blair (CDF Collaboration), These proceedings.
7. F. Abe *et al.* (CDF Collaboration), *Phys. Rev. Lett.* **72**(1994)3005.
8. P. Rubinov (D0 Collaboration), DPF94, Fermilab-Conf-94/323B-E.
9. F. Abe *et al.* (CDF Collaboration), *Phys. Rev. Lett.* **71**(1993)679.
10. F. Abe *et al.* (CDF Collaboration), *Phys. Rev. Lett.* **62**(1989)3020; R. Harris, (CDF Collaboration), Proceedings of the XXIXth Recontres de Moriond (1994), Fermilab-Conf-94/101-E.